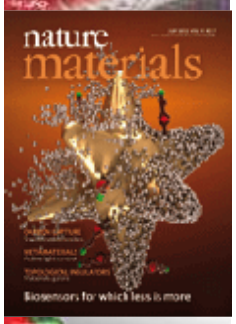

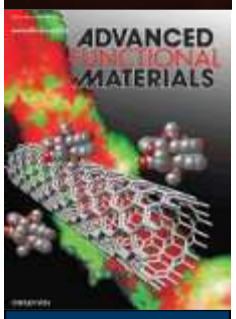

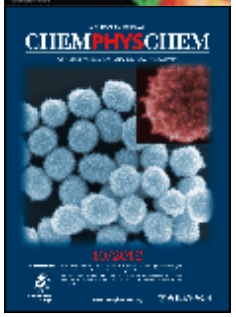

Colloid Chemistry Group

BiO NanoPlasmOnics

CIC biomaGUNE
Biomaterialetako Ikerkuntza Kooperatibako Zentroa
Centro de Investigación Cooperativa en Biomateriales

2013

BioNanoPlasmonics Lab

January **2013**

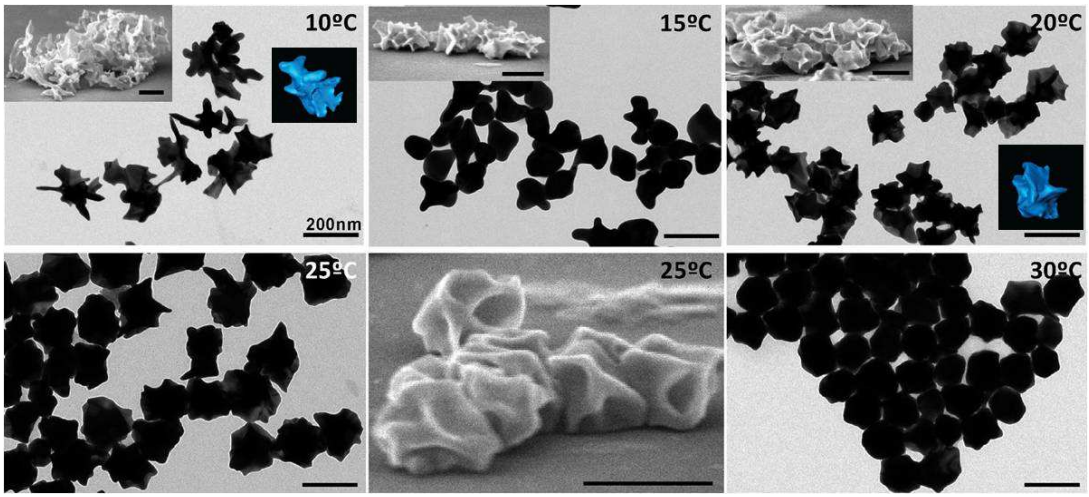

Seedless Synthesis of Single Crystalline Au Nanoparticles with unusual shapes and localized surface Plasmon resonances in the near-infrared. Cetyltrimethylammonium chloride (CTAC) was used to induce the seedless formation of highly anisotropic, twisted single crystalline Au nanoparticles in a single step. The image above shows TEM and SEM micrographs of the Au nanoparticles obtained at different temperatures, as indicated in the labels. In all cases [Au]:[CTAC]:[AA] = 1:60:16. All scale bars correspond to 200 nm. Blue insets correspond to 3D electron tomography images, along different viewing directions. *Chem. Mater.* **2012**, *24*, 1393−1399.

Monday	Tuesday	Wednesday	Thursday	Friday	Saturday	Sunday
	1	2	3	4	5	6
7	8	9	10	11	12	13
14	15	16	17	18	19	20
21	22	23	24	25	26	27
28	29	30	31			

February **2013**

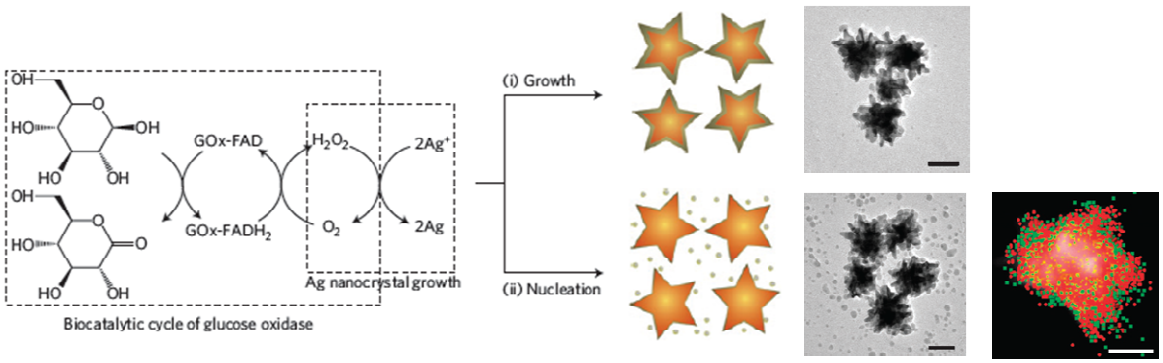

Plasmonic nanosensors with inverse sensitivity by means of enzyme-guided crystal growth. The image shows a Scheme of the proposed signal-generation mechanism by means of enzyme-guided crystal growth. GOx generates hydrogen peroxide, which reduces silver ions to grow a silver coating around plasmonic nanosensors (gold nanostars); (i) at low concentrations of GOx the nucleation rate is slow, which favours the growth of a conformal silver coating that induces a large blue-shift in the localized surface plasmon resonance (LSPR) of the nanosensors; (ii) when GOx is present at high concentrations, the fast crystal growth conditions stimulate the nucleation of silver nanocrystals and less silver is deposited on the nanosensors, therefore generating a smaller variation of the LSPR. When the concentration of GOx is related to the concentration of a target molecule through immunoassay, this signal-generation step induces inverse sensitivity because condition (i) is fulfilled at low concentrations of analyte. FAD and FADH2 are the oxidized and reduced forms of flavin adenine dinucleotide. TEM pictures after the signal-generation step when gold nanostars were modified with 10^{-20} g ml^{-1} GOx (**a**) and 10^{-14} g ml^{-1} GOx (**b**); scale bars, 50 nm. XEDS map showing the distribution of gold (red) and silver (green) around nanostars, scale bar, 20 nm. *Nature Materials*, **2012**, *11*, 604-607.

Monday	Tuesday	Wednesday	Thursday	Friday	Saturday	Sunday
				1	2	3
4	5	6	7	8	9	10
11	12	13	14	15	16	17
18	19	20	21	22	23	24
25	26	27	28			

March **2013**

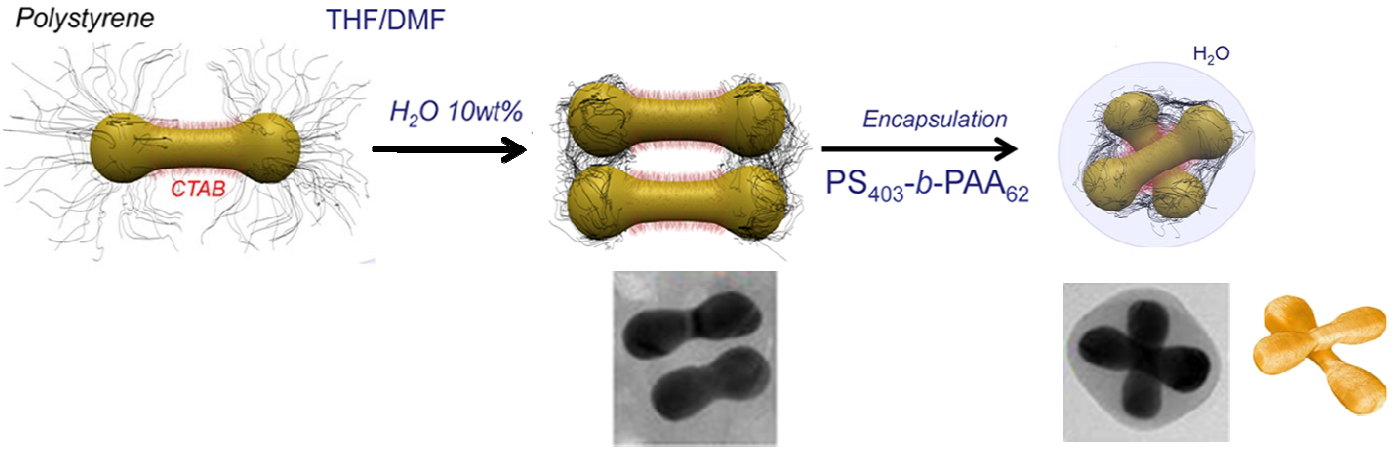

Steric Hindrance Induces crosslike Self-Assembly of Gold Nanodumbbells. We have shown that the combination of patchiness (attraction) and shape (steric hindrance) allows assembling gold nanodumbbell building blocks into crosslike dimers with well-controlled interparticle distance and relative orientation. The image above shows how polystyrene-stabilized particles undergo gradual clustering upon addition of water to THF/DMF solution, and finally encapsulation of clusters inside polymeric micelles induces the crosslike morphology. Below the schematic representation, TEM image of crosslike dimmers and three-dimensional electron tomography reconstruction of clusters encapsulated in polymeric micelles can be observed. *Nano Lett.* **2012**, *12*, 4380−4384.

Monday	Tuesday	Wednesday	Thursday	Friday	Saturday	Sunday
				1	2	3
4	5	6	7	8	9	10
11	12	13	14	15	16	17
18	19	20	21	22	23	24
25	26	27	28	29	30	31

April **2013**

Silica-coated GNRs

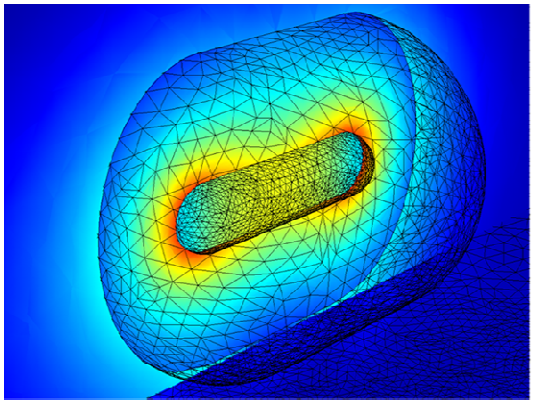

Bare GNRs

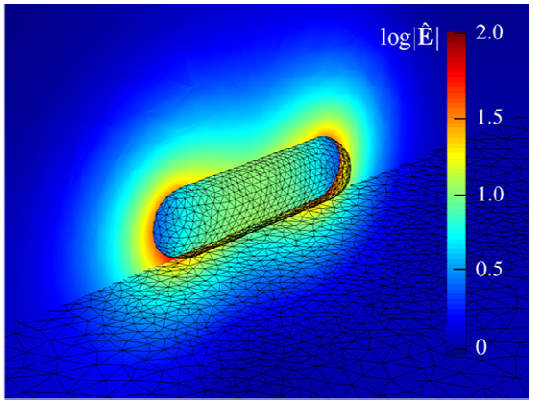

Effects of the dielectric environment on the optical extinction spectra of gold nanorods. The optical extinction spectra of single bare and silica-coated gold nanorods were quantitatively measured around their longitudinal SPR using spatial modulation spectroscopy, and the results were compared to those of a numerical model of optical absorption. The combination of these experimental and theoretical methods constitutes a powerful tool for the detailed interpretation of the optical properties of single nanoparticles. The image above shows plots of the relative electric field, $\hat{E} = |E|/|E_{inc}|$, where $|E| = (E \cdot E^*)^{1/2}$ is the amplitude of the total electric field and E_{inc} is the amplitude of the incident field. Superimposed on this is the surface discretization of the gold, silica coating, and substrate regions. $\hat{E}$ is shown on a color log-scale. Therefore red represents a field amplification of 100×, cyan represents an amplification of 10×, and dark blue represents a field amplitude equal to the incident field. The GNR shown was approximately 33 nm long. *ACSNano*, **2012**, *6*, 8183-8193.

Monday	Tuesday	Wednesday	Thursday	Friday	Saturday	Sunday
1	2	3	4	5	6	7
8	9	10	11	12	13	14
15	16	17	18	19	20	21
22	23	24	25	26	27	28
29	30					

May **2013**

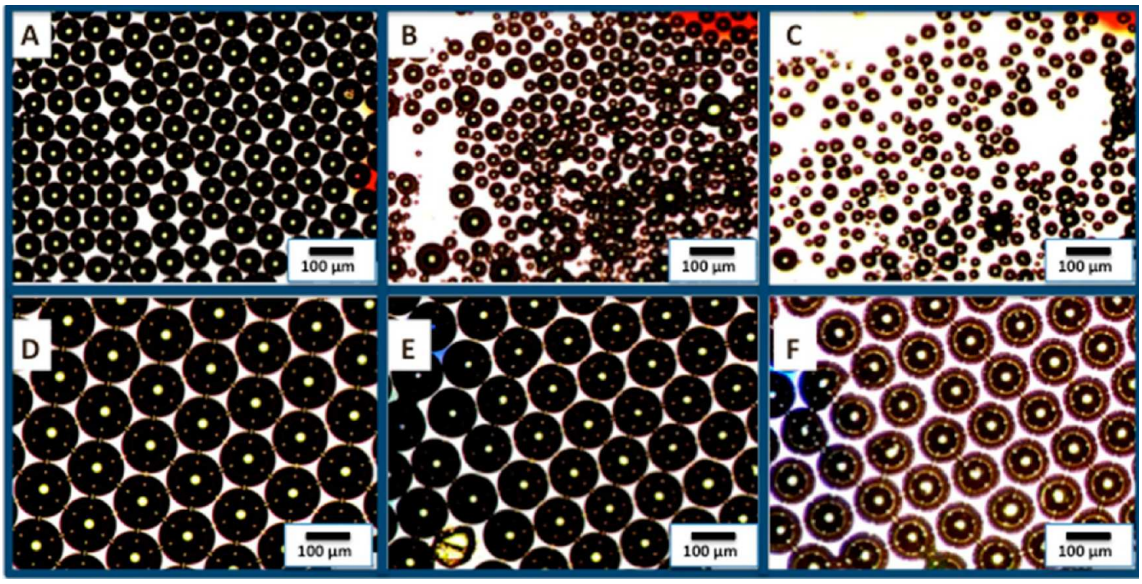

Effects of Gold Nanoparticles on the Stability of Microbubbles. Microbubbles prepared from a liquid suspension of gold nanoparticles were found to have significantly enhanced stability compared with bubbles coated only with surfactant. The former remained monodisperse for upward of 72 h and stable for 30 days compared with 24 h for the latter. The image above shows a comparison of the stability of surfactant coated microbubbles without (A–C) and with the addition of gold nanoparticles (D–F). *Langmuir* **2012**, 28, 13808–13815.

Monday	Tuesday	Wednesday	Thursday	Friday	Saturday	Sunday
		1	2	3	4	5
6	7	8	9	10	11	12
13	14	15	16	17	18	19
20	21	22	23	24	25	26
27	28	29	30	31		

June **2013**

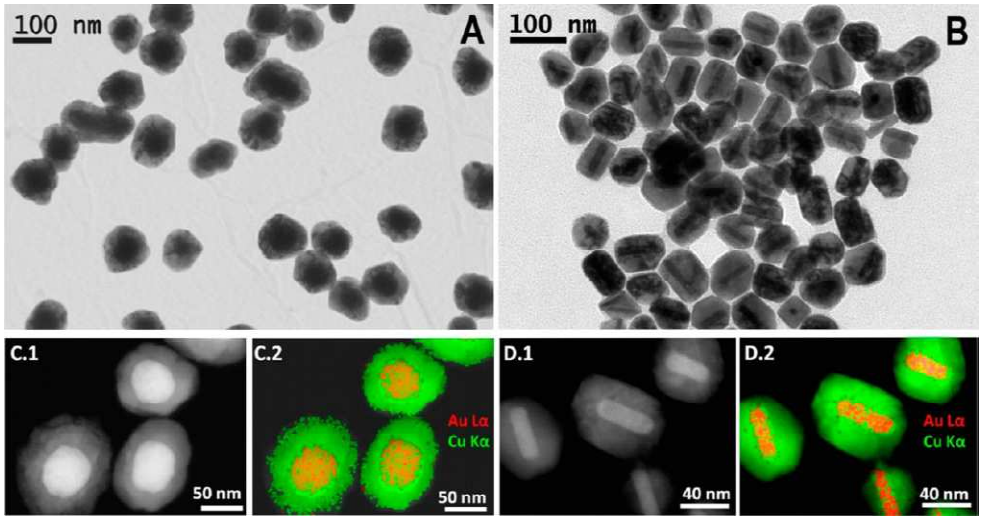

Shape-Templated Growth of Au@Cu Nanoparticles. The seed mediated method can be used to grow Cu nanoparticles with controlled size and morphology, determined by Au nanoparticle seeds, thus allowing surface Plasmon resonance tuning. The image above shows representative TEM micrographs of core–shell Au@Cu nanoparticles obtained using as seeds (PEG)-capped Au polycrystalline spheres (57.0 ± 7.6 nm diameter) and single crystal nanorods (65.7 ± 8.5 nm long, 13.7 ± 2.3 nm thick). (C.1, D.1) HAADF STEM images showing mass–thickness contrast.(C.2, D.2) STEM-XEDS elemental maps (Au = red; Cu = green). *J. Phys. Chem. C*, DOI: 10.1021/jp3062724.

Monday	Tuesday	Wednesday	Thursday	Friday	Saturday	Sunday
					1	2
3	4	5	6	7	8	9
10	11	12	13	14	15	16
17	18	19	20	21	22	23
24	25	26	27	28	29	30

July **2013**

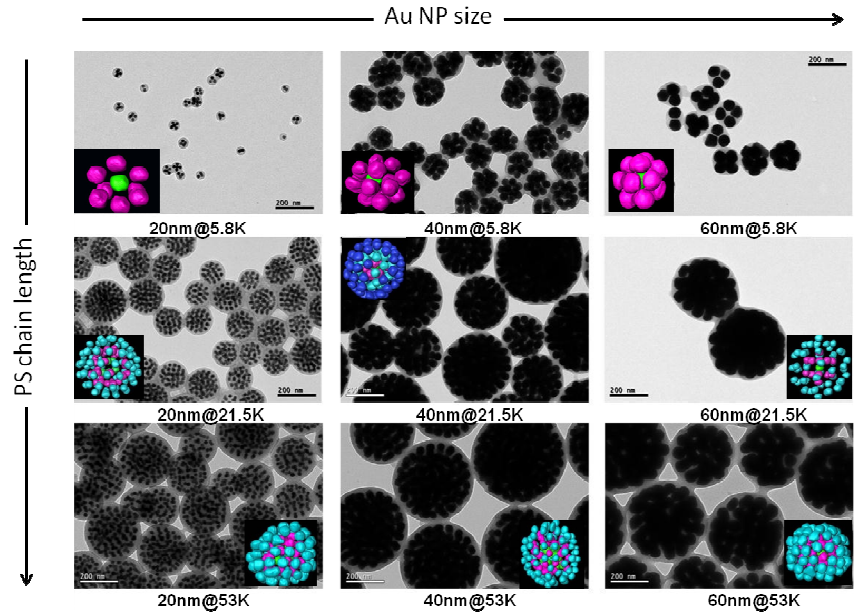

Hydrophobic interactions modulate self-assembly of nanoparticles. We have described a general methodology for solvent-induced, reversible self-assembly of gold nanoparticles into 3D clusters with well-controlled sizes. As shown in the image above, the size of the clusters can be controlled by the molecular weight of the grafted polystyrene chains. With increasing the length of the polymer chains the size of the clusters increases. The coloured insets show electron tomography reconstructions of clusters. *ACSNano*, **2012**, *6*, 11059-11065.

Monday	Tuesday	Wednesday	Thursday	Friday	Saturday	Sunday
1	2	3	4	5	6	7
8	9	10	11	12	13	14
15	16	17	18	19	20	21
22	23	24	25	26	27	28
29	30	31				

August **2013**

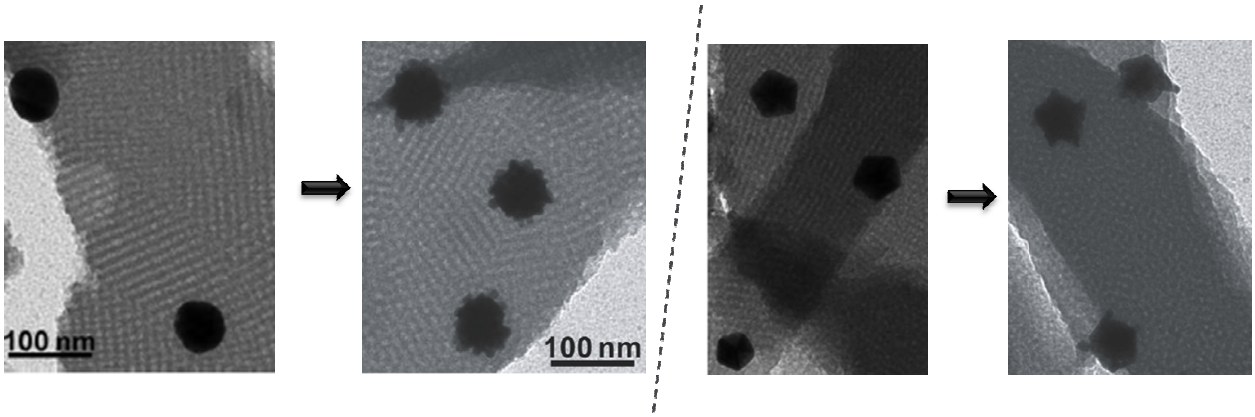

Growth and branching of gold nanoparticles through mesoporous silica thin Films. We have shown the fabrication of composite materials containing a sub-monolayer of gold nanoparticles (GNPs) of various shapes covered with mesoporous silica thin films. Additionally, the shape of the GNPs (and thus their optical properties) can be modified in situ through seeded growth and branching. The final shape of the GNPs was also found to depend on their initial shape and size, as well as the pore size of the mesoporous film covering them. Because the growth proceeds through the pores of the film, it may lead to shapes that are not easily obtained in solution, such as particles with branches on one side only. The image above shows representative TEM micrographs of S_{60}@SF (left) and D@SF (right) before and after grown with CTAB : AA : Au solution with 60 : 16 : 1 molar ratio. *Nanoscale* **2012**, *4*, 931-939.

Monday	Tuesday	Wednesday	Thursday	Friday	Saturday	Sunday
			1	2	3	4
5	6	7	8	9	10	11
12	13	14	15	16	17	18
19	20	21	22	23	24	25
26	27	28	29	30	31	

September **2013**

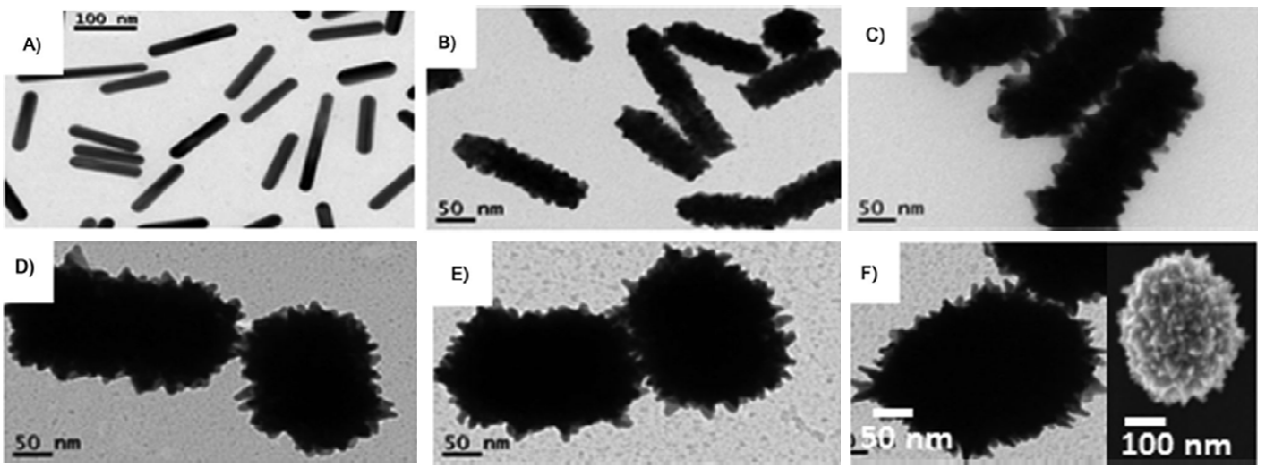

Spiked Gold Beads as Substrates for Single-Particle SERS. We demonstrated that the antenna effect from the cores in Au spiked beads results in higher SERS signals for colloids and that the signal intensity is increasing with the core size of the particles. In the figure above, representative TEM images of the particles resulting from seeded growth of gold nanorods (A, aspect ratio: 5) with different [HAuCl4]/[seed] ratios: B) 5.5; C) 22; D) 55; E) 90; and F) 130. *ChemPhysChem* **2012**, *13*, 2561 – 2565.

Monday	Tuesday	Wednesday	Thursday	Friday	Saturday	Sunday
						1
2	3	4	5	6	7	8
9	10	11	12	13	14	15
16	17	18	19	20	21	22
23	24	25	26	27	28	29
30						

October **2013**

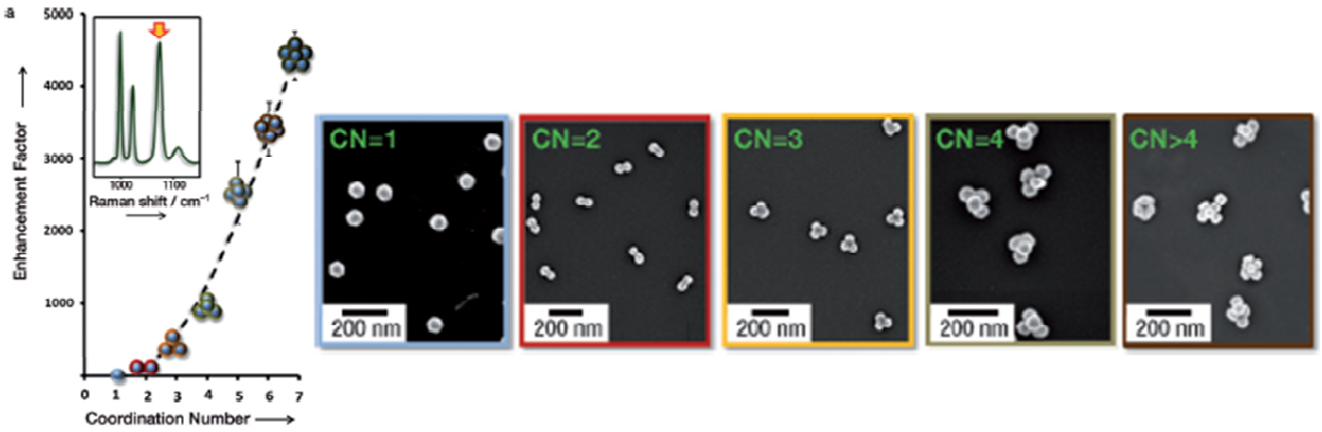

Organized Plasmonic Clusters with High Coordination Number and Extraordinary Enhancement in Surface-Enhanced Raman Scattering (SERS). In summary, we have shown that by using a polymeric coating and emulsion clustering it is possible to produce plasmonic nanoparticle molecules with high symmetry and coordination index, which can be separated by applying density gradient centrifugation. Narrow interparticle gaps are produced with subsequent strong optical interactions while allowing the analytes to diffuse inside the gaps, where gigantic electric fields are generated, as we have shown by directly measuring the SERS enhancement in the clusters. The image shows a comparison between the enhancement factors obtained for each sample, normalized to the enhancement produced by a single particle excited with a 633 nm laser line. Inset: SERS spectra of benzenethiol on the pentagonal bipyramid (CN 7). The SEM micrographs correspond to the different cluster populations obtained after careful density gradient separation. *Angew. Chem. Int. Ed.* **2012**, *51*, 12688 –12693.

Monday	Tuesday	Wednesday	Thursday	Friday	Saturday	Sunday
	1	2	3	4	5	6
7	8	9	10	11	12	13
14	15	16	17	18	19	20
21	22	23	24	25	26	27
28	29	30	31			

November **2013**

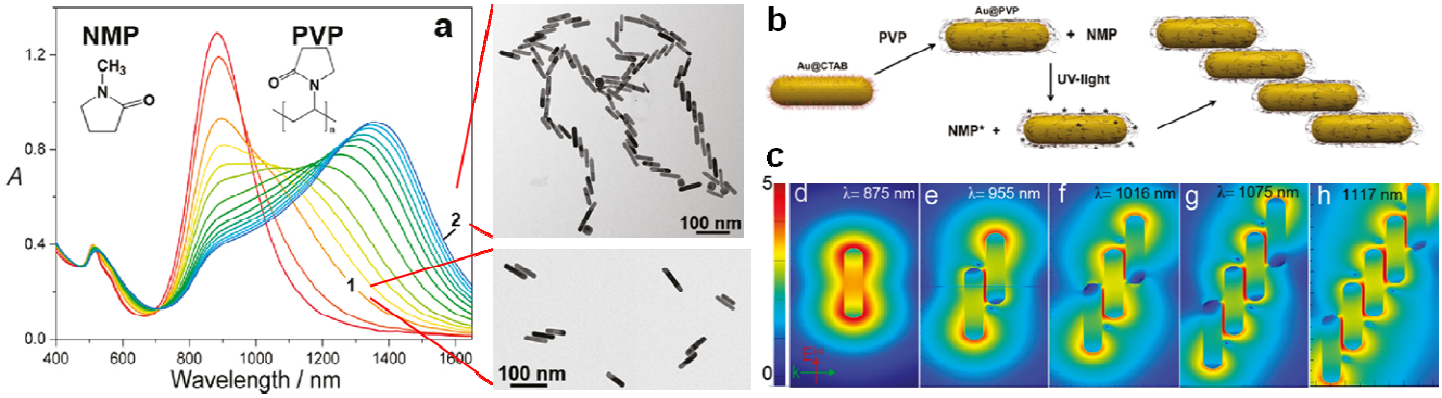

Antibonding Plasmon Modes in Colloidal Gold Nanorod Clusters. We found that UV−light irradiation of colloidal dispersions of AuNRs in N-methyl-2-pyrrolidone (NMP), stabilized by poly(vinylpyrrolidone) (PVP) results in the creation of AuNRs clusters with ladderlike morphology, where antibonding modes can be identified(b). In the image, the UV−vis-NIR spectra shows the changes in the longitudinal LSPR band over time. TEM images demonstrating the formation of assemblies at different elapsed times: 5 h, corresponding to spectrum 1 and 25 h, corresponding to spectrum 2. (c) Electric near field enhancement maps for clusters of increasing number of AuNR units, at their corresponding LSPR maximum wavelength. The direction and polarization of incident light are indicated in the first image. *Langmuir* **2012**, *28*, 8826–8833.

Monday	Tuesday	Wednesday	Thursday	Friday	Saturday	Sunday
				1	2	3
4	5	6	7	8	9	10
11	12	13	14	15	16	17
18	19	20	21	22	23	24
25	26	27	28	29	30	

December **2013**

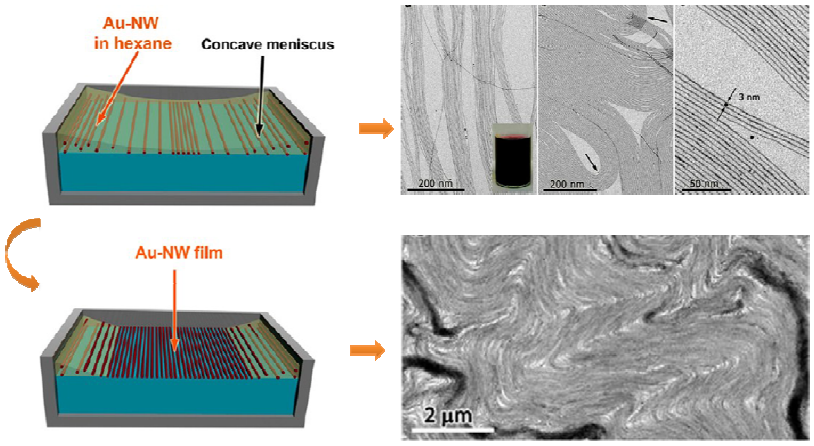

Highly Transparent and Conductive Films of Densely Aligned Ultrathin Au Nanowire Monolayers. We have reported a facile method to prepare single layers of densely aligned ultrathin Au-nanowires, homogeneous over cm² areas. The as deposited films show an electrical/optical performance competitive with ITO and graphene-based electrodes. The image above shows a Schematic diagram of the Au-DANW monolayer film formation. Transmission electron microscopy (TEM) images (upper) of the as-prepared Au-NWs deposited on a TEM-grid and of a typical Au-NW solution and (lower) of a self-assembled monolayer thick Au-NW deposited on a carbon-coated Ni TEM grid. *Nano Lett.*, **2012**, *12*, 6066-6070.

Monday	Tuesday	Wednesday	Thursday	Friday	Saturday	Sunday
						1
2	3	4	5	6	7	8
9	10	11	12	13	14	15
16	17	18	19	20	21	22
23	24	25	26	27	28	29
30	31					

2013

BioNanoPlasmonics Lab